Phytoplanktonic species in the haloalkaline Lake Dziani Dzaha select their archaeal microbiome

Maxime Bruto, Phil M. Oger, Patrice Got, Cécile Bernard, Delphine Melayah, Lilian Cloarec, Charlotte Duval, Arthur Escalas, Sébastien Duperron, Ludivine Guigard, et al.

Phytoplanktonic species in the haloalkaline Lake Dziani Dzaha select their archaeal microbiome

Bruto M[1], Oger P.M.[2], Got P[3], Bernard C[4], Melayah D[2], Cloarec L.A.[2], Duval C[4], Escalas A[3], Duperron S[4], Guigard L[2], Leboulanger C[3], Ader M[5], Sarazin G[5], Jézéquel D[5,6], Agogué H[7], Troussellier M[3], Hugoni M[2,8]

[1] VetAgro Sup, Anses, UMR Mycoplasmoses Animales, F-69280 Marcy l'Etoile, France

[2] INSA Lyon, Universite Claude Bernard Lyon 1, CNRS, UMR5240 Microbiologie Adaptation et Pathogénie, F-69621 Villeurbanne, France

[3] MARBEC, Univ Montpellier, IRD, CNRS, Ifremer, Sète, France

[4] UMR 7245 Molécules de Communication et Adaptations des Microorganismes (MCAM) MNHN-CNRS, Muséum National d'Histoire Naturelle, CP 39, 12 rue Buffon, F-75231 Paris Cedex 05, France

[5] Institut de Physique du Globe de Paris, Université Paris Cité, CNRS, F-75005 Paris, France

[6] UMR CARRTEL, INRAE-USMB, Thonon, France

[7] LIENSs, UMR7266, La Rochelle Université - CNRS, La Rochelle, France

[8] Institut Universitaire de France (IUF)

Corresponding author: Mylène Hugoni, Universite Claude Bernard Lyon 1, INSA Lyon, CNRS, UMR5240 Microbiologie Adaptation et Pathogénie, F-69621 Villeurbanne, France - mylene.hugoni@univ-lyon1.fr

ORCID: 0000-0002-2430-1057

Running head: Archaeal phycospheric microbiome

Keywords: Phycosphere, microscale, microbial diversity, archaea, thalassohaline ecosystem

Abstract

Microorganisms are key contributors of aquatic biogeochemical cycles, but their microscale ecology remains largely unexplored, especially interactions occurring between phytoplankton and microorganisms in the phycosphere, *i.e.,* the region immediately surrounding phytoplankton cells. The current study aimed to provide evidence of the phycosphere taking advantage of a unique hypersaline, hyperalkaline ecosystem, Lake Dziani Dzaha (Mayotte), where two phytoplanktonic species permanently co-dominate: a cyanobacterium, *Arthrospira fusiformis*, and a green microalga, *Picocystis salinarum.* To assay phycospheric microbial diversity from *in situ* sampling, we set up a flow cytometry cell-sorting methodology for both phytoplanktonic populations, coupled with metabarcoding and comparative microbiome diversity. We focused on archaeal communities as they represent a non-negligible part of the phycospheric diversity, however their role is poorly understood. This work is the first which successfully explores *in situ* archaeal diversity distribution showing contrasted phycospheric compositions, with *P. salinarum* phycosphere notably enriched in Woesearchaeales OTUs while *A. fusiformis* phycosphere was enriched in methanogenic lineages affiliated OTUs such as Methanomicrobiales or Methanofastidiosales. Most archaeal OTUs, including Woesearchaeales considered in literature as symbionts, were either ubiquitous or specific of the free-living microbiome (*i.e.*, present in the 3-0.2µm fraction). Seminally, several

archaeal OTUs were enriched from the free-living microbiome to the phytoplankton phycospheres, suggesting (i) either the inhibition or decrease of other OTUs, or (ii) the selection of specific OTUs resulting from the physical influence of phytoplanktonic species on surrounding Archaea.

Introduction

Microorganisms, including bacteria, microeukaryotes and archaea drive and supply many ecological processes especially through their interactions (Allison & Martiny, 2008; Liu et al., 2019). Interactions conditioning the structure and dynamics of microbial communities (Cordero & Datta, 2016; Orland et al., 2020) take place within micrometre-scale (*i.e.* microscale) cell aggregates and only in a short-range of a few cell diameters (Dal Co et al., 2020). However, the microbial interactions occurring at this scale and their consequences for ecosystem functioning, stability and resilience remain largely unexplored.

In aquatic ecosystems, the production and maintenance of high phytoplanktonic biomass, as observed during blooms, does not depend solely on the functional capabilities of the dominant species but also on the interactions they are engaged in (Woodhouse et al., 2016; Yang et al., 2017). These interactions mainly take place in the intimate zone of molecule exchanges between bacterial and archaeal communities and phytoplanktonic cells (Bell & Mitchell, 1972), *i.e.* the phycosphere. This microscale region, analogous to the plant root rhizosphere, serves as the interface for phytoplankton and their microbiome interactions.

Most of these interactions are based on the release by the host cell of exudates that fuel their heterotrophic microbiome, which in turn can either release growth hormones and

vitamins (Amin et al., 2015; Croft et al., 2005) to stimulate phytoplanktonic species, or protecting them from pathogens (Seyedsayamdost et al., 2014) or facilitate their iron uptake (Amin et al., 2009). It has been shown that this nutrient dependence relies upon the functional complementarity of the species involved (Halary et al., 2022; Pascault et al., 2021), which has been engineered over evolutionary times by the host cells. Moreover, the class of metabolites exudated by phytoplanktonic species can influence the phycosphere microbiome composition (Fu et al., 2020; Shibl et al., 2020). While recent works suggested that the phycosphere contains many new and undiscovered microbial lineages and genetic resources (Ashraf et al., 2023; Zhang et al., 2019), few investigated the phycospheric microbiome considering bacteria, microeukaryotes and archaea simultaneously. Moreover, classical studies target the phycosphere, considered as a particle-attached-fraction, through cultivation of large algae (from 8 to 200µm), mesocosms or gradual filtration (Halary et al., 2022; Sapp et al., 2007; Zhou et al., 2019) showing that particle-attached and free-living microbiomes exhibit different taxonomic composition, physiology and metabolism corresponding to their lifestyle and ecological behavior (Li et al., 2021, Suzuki et al., 2017, Yang et al., 2017).

Lake Dziani Dzaha (Mayotte, Indian Ocean) is an extreme thalassohaline, hypersaline, hyperalkaline lake characterized by many unique geochemical and biological features (Leboulanger et al., 2017; Sarazin et al., 2021). One of these features is the high and stable chlorophyll *a* concentration over time (mean concentrations ranging from 566 to 702 $\mu g.L^{-1}$, reported over the 2010-2015 period (Leboulanger et al., 2017), 587 $\mu g.L^{-1}$ in 2018), which is of great interest in the study of phytoplanktonic phycosphere compared with other ecosystems where phytoplanktonic blooms occurs only periodically. In temperate areas where cyanobacterial blooms occur in lakes, they only appear during the

summer period (Louati et al., 2023). Indeed, whatever the season, the cyanobacterium *Arthrospira fusiformis* and the picoeukaryotic algae *Picocystis salinarum* dominate the phototrophic microbial assemblage (Bernard et al., 2019) in the two main contrasted ecological niches of the water column: the photic upper layer (i.e. above 2 m), where oxygen and light were detected and the aphotic, anoxic deeper layer (i.e. below 2 m) (Bernard et al., 2019; Hugoni et al., 2018; Leboulanger et al., 2017), presenting high concentrations in H_2S/HS^-, pH values higher than 9 and salinities exceeding 60 psu (Leboulanger et al., 2017; Sarazin et al., 2021). This co-dominance contrasts with the dominance of a single successful species as observed in other hypersaline lakes (Dadheech et al., 2013; Krienitz et al., 2013; Sorokin et al., 2014) and is likely due to differences in their pigment composition (Bernard et al., 2019) and the ability of *P. salinarum* to adapt to low light intensity (Pálmai et al., 2020; Roesler, 2002). Although a sharp decrease of *A. fusiformis* and *P. salinarum* abundances along the water column depth has been reported (Bernard et al., 2019) associated to an unknown physiological status, it does not result from grazing by aquatic metazoans as these are absent from the lake (Hugoni et al., 2018).

While the phycospheric diversity is suspected to be important for phytoplankton life cycle, allowing niche protection, nutrient and/or metabolite exchanges with the phototrophic cells (through exudates consumption, chemotaxis, etc.), the microbiome associated with the dominant phytoplanktonic species, *A. fusiformis* and *P. salinarum* has not been identified yet. Despite much larger size, *A. fusiformis* (filaments average length 335 µm [min 170 µm - max 2,390 µm] (Cellamare et al., 2018)) appears to co-occur with a very limited number of archaeal and bacterial taxa (OTUs) compared to *P. salinarum* (diameters from 2.5 to 4.5 µm (Cellamare et al., 2018)), according to co-occurrence microbial networks (CMN) (Escalas et al., 2021). This counter-intuitive observation

advocates for a high selectivity in *A. fusiformis* phycosphere and the possible lack of a specific *P. salinarum* phycosphere for which the detected microbiome might only reflect the free-living communities in the vicinity of the cells. The hypothesis of an absence of a *P. salinarum* phycosphere by Escalas *et al.* (2021) was congruent with predictions suggesting that chemotactic associations could not be detected for phytoplanktonic cells smaller than 4 µm (J. R. Seymour et al., 2017). However, associations between taxa identified using CMN correspond to statistical relationships that are observed at a relatively large observational scale compared with the scale at which microbial interactions do actually occur, being relevant for the phycosphere study.

Here, we used a cell-level observational scale, based on flow cytometry cell-sorting, to test the existence of specific phycospheric microbiomes (*i.e.* particle-attached), hypothesized previously at larger scale (Escalas et al., 2021), for the two-codominant phytoplanktonic species, *A. fusiformis* and *P. salinarum*, retrieved in the same ecosystem, Lake Dziani Dzaha. We investigated the diversity of bacterial, microeukaryotic and archaeal communities retrieved within the phycosphere of the two primary producers to test whether these two phytoplanktonic species harbor specific phycospheric microbiomes. By comparing the phycosphere microbiomes with the surrounding water free-living microbiome (3-0.2µm fraction), we evidenced (1) distinct microbiomes composition in the phycospheres (particle-attached) *versus* the free-living fraction (non-phycospheric), (2) the presence of unexpected archaeal phycosphere communities for *P. salinarum* which were different in OTUs and sequence abundance from the free-living fractions. (3) We evidenced the selection of specific archaeal OTUs by the phytoplanktonic cells to thrive in their intimacy.

Materials and Methods

Study site, sampling, and environmental parameters

Lake Dziani Dzaha is a volcanic crater lake located in the Comoros archipelago (Western Indian Ocean) on the Petite Terre Island of Mayotte (12°46′ 15.6″ S; 45° 17′ 19.2″ E; Latitude: -12.771, Longitude: 45.2887). The lake surface is approximately 0.24 km^2 with a mean depth of ~3.5 m except for the eastern part of the lake where a narrow pit reaching a maximum depth of 18 m is present. The elevation of the lake surface is close to the average sea level. This lake is characterized by a higher-than-seawater salinity (ranging from 34 to 71 psu), a strong alkalinity (0.23 mol L^{-1}) and a permanent green color due to a high primary production (Leboulanger et al., 2017). Eight water samples (1.2 L) were collected on November 14th, 2018, along a depth profile (0.25 m, 1 m, 1.5 m, 2.5 m, 5 m, 11 m, 14 m and 16 m) located above the deepest point of the lake, using a horizontal Niskin bottle, and were processed within 2 hours following collection. Because of the clogging effect, to collect the free-living microbiome, a 45 mL subsample was filtered successively through 3-µm and 0.2-µm (30 mL) pore-size polycarbonate filters. The filters were stored at -20°C until nucleic acid extraction was performed. Another 250 mL water subsample was stored at room temperature in the dark in Nalgene bottles until cell-sorting by flow cytometry performed from November 20th to 23rd, 2018 (+ 4-7 days). Vertical profiles for pH, dissolved O_2, temperature and conductivity were measured using a WTW 3630 probe. The salinity was calculated based on conductivity and temperature. Chl *a* was analyzed after extraction using 96% ethanol by ultrasonication in an ice bath for 30 sec, and further extraction was allowed overnight at 4 °C in the dark. The extract was filtered, and the

filtrate was analyzed spectrophotometrically at 400–750 nm. The concentration of Chl *a* was calculated according to Ritchie (Ritchie, 2006).

Flow cytometry cell-sorting

The workflow for flow cytometry cell-sorting was determined as a compromise of different requirements (i) the amount of DNA needed to prepare libraries, (ii) the efficiency of *A. fusiformis* and *P. salinarum* cell-sorting, and (iii) the time necessary to perform the experimentation, which should not affect microbial diversity.

Autotrophic populations consisting of *Picocystis salinarum* and *Arthrospira fusiformis* were sorted using a FACS Aria Flow cytometer (Becton Dickinson, San Jose, CA, USA), equipped with a blue laser (488nm), following the procedure described in Figure S1. Our working hypothesis is that the microbial members present in the phycosphere of *P. salinarum* and *A. fusiformis* were sorted concomitantly with the phytoplanktonic populations as they are closely associated with them.

Samples were pre-filtered on a 20µm sieve and sorting parameters were: nozzle of 70µm (70PSI) with Facs flow (stream) and BD FACSDiva software: amplitude: 88 Mhz voltage sorting 5v, the Drop Delay: 38.4 µs and GAP = 6 pixels. The sorting quality (fine tube) using accudrop beads (BD) for 1600 to 2000 events/s, was obtained with a sorting efficiency percentage > to 95%. The procedure allowed to sort about 10^6 events for *P. salinarum*, and 5000 events for *A. fusiformis*, Figure S2 and Table S1) in a limited time (2h) to prevent any alteration of the sorted cells. *P. salinarum* and *A. fusiformis* cells were excited at 488 nm and sorted on parameters depending on their FALS and RALS properties and red fluorescence (>650 nm) from chlorophyll pigments. The sorted cells were collected

187 in a polypropylene tube containing 500 µl of Dziani Dzaha lake water, which was filtered
188 at 0.2 µm and heated to 60°C to denature viral particles beforehand.
189
190 ***DNA extraction, Illumina sequencing and sequence processing***
191 DNA extractions were performed on the free-living fraction (*i.e.* 0.2µm filters) using the
192 ZymoBIOMICS DNA Miniprep kit (Zymo Research) following the manufacturer's
193 recommendations but amended with a phenol/chloroform/isoamyl alcohol (25:24:1) step to
194 further purify the DNA. DNA quality was checked by 1% (w/v) agarose gel electrophoresis
195 and quantified using NanoDrop (Table S1). The same extraction procedure was used for
196 flow cytometry cell-sorted fractions (Table S1).
197 The V3-V5 region of the 16S rRNA genes was amplified in triplicate for *Bacteria*
198 and *Archaea* using the universal primers 357F (Schuurman et al., 2004) and 926R (Walters
199 et al., 2016) and 519F and 915R (Hugoni et al., 2015), respectively (Table S2). For
200 Eukaryota, the V4 region of the 18S rRNA genes was amplified in triplicate using the
201 universal primer 515F (Caporaso et al. 2011) and the eukaryotic primer 951R (Lepère et al.,
202 2016) (Table S2). Additionally, a DNA extraction was carried out in absence of biological
203 matrix to obtain a negative control of lab-induced contamination. High-throughput
204 sequencing was achieved after pooling PCR triplicates and performing a multiplexing step
205 using MiSeq 300 bp PE technology (Biofidal, Vaulx-en-Velin, France -
206 http://www.biofidal-lab.com).
207 Bacterial and archaeal 16S rRNA and eukaryotic 18S rRNA paired-end reads were
208 merged with a maximum of 10% mismatches in the overlap region using VSEARCH
209 (Rognes et al., 2016). Denoising procedures consisted of discarding reads containing
210 ambiguous bases (N) or reads outside the range of expected length (*i.e.*, 450 to 580 bp for

bacterial 16S rRNA genes, 370 to 580 bp for archaeal 16S rRNA genes, and 250 to 420 bp for eukaryotic 18S rRNA genes). After dereplication, sequences were clustered using SWARM (Mahé et al., 2014) with a local clustering threshold. Chimeric OTUs were removed with VSEARCH (Rognes et al., 2016) and along with OTUs representing less than 0.005% of the total number of sequences (Bokulich et al., 2013) and singletons. The eukaryotic dataset was cured of eukaryotic contaminations (higher metazoan sequences) to create the microeukaryotic dataset. Taxonomic assignment was performed with both RDP Classifier (Wang et al., 2007) and BLASTN+ (Camacho et al., 2009) against the 138.1 SILVA database (Pruesse et al., 2007). This procedure was automated in the FROGS pipeline (Escudié et al., 2017). Contaminant Operational Taxonomic Units (OTUs) identified from the control samples were removed. Last, samples were randomly resampled to allow comparisons between samples, Table S3).

Statistical analyses

For each sample, richness (Chao-1) and diversity (Shannon) indices were computed using the VEGAN package (http://cran.r-project.org/web/packages/vegan/index.html) in R. Distribution of OTUs among the different conditions was illustrated with Venn diagrams (http://bioinformatics.psb.ugent.be/webtools/Venn/). An ordination of the samples was realized using NMDS approach based on Jaccard index computed from presence-absence matrices and on Bray-Curtis dissimilarity computed from sequence abundance data (function *metaMDS* in R). A stress value was calculated to measure the difference between the ranks on the ordination configuration and the ranks in the original similarity matrix for each repetition (Ramette, 2007). An acceptable stress value should be below 0.2. An analysis of similarity (ANOSIM) was calculated to test the differences between each

fraction and to further confirm the results observed in the NMDS plot. These analyses were performed with the VEGAN package (http://cran.r-project.org/web/packages/vegan/index.html) in R.

Archaeal phylogeny

Archaeal OTUs sequences retrieved in the *A. fusiformis* and *P. salinarum* phycospheres and in the free-living microbiome were extracted for the three datasets and aligned using MAFFT (Kuraku et al., 2013). Gaps and poorly conserved regions were eliminated using Gblocks (Castresana, 2000; Talavera & Castresana, 2007). The phylogeny was reconstructed using fastme 2.1.5 (Lefort et al., 2015), with the F84 nucleotide model and NNI+SPR topological optimization under the balanced minimum evolution principle. Node support was estimated using the bootstrap method (1000 replicates). The tree was visualized together with the presence/absence matrix of OTUs in the *A. fusiformis* and *P. salinarum* phycospheres and in the free-living microbiome, using iTOL (https://itol.embl.de).

Results

Physico-chemical properties of the water column

Physico-chemical parameters recorded during November 2018 indicated that the water column was not stratified in terms of salinity, pH and temperature (Figure 1). It was however stratified in terms of O_2 saturation, with an oxycline between 0.25 and 1m, where O_2 saturation decrease from 89.9% to 21.7%, and anoxic waters at depth, with 0% O_2 saturation at 11m depth.

Flow-cytometry cell-sorting methodological validations

The microscale resolution of the present work implies that DNA extracted from cell sorted fractions was at least ~ten-fold magnitude lower as compared to DNA retrieved from the filtered water samples that correspond to upstream and downstream cell sorting controls (Table S1). Hence, an average of 2.4 $ng.\mu L^{-1}$ of DNA in the *A. fusiformis* panel and 3.6 $ng.\mu L^{-1}$ in the *P. salinarum* panel were obtained, which contrasted with the average 46.8 and 49.1 $ng.\mu L^{-1}$ of DNA extracted from the unsorted 20-0.2µm fractions.

Nonetheless, in the bacterial dataset, a clear enrichment in *P. salinarum* mitochondrion and chloroplast sequences (i.e. 16S rRNA genes) in the *P. salinarum* phycosphere associated with an increase in *A. fusiformis* sequences in the *A. fusiformis* phycosphere fraction demonstrated the cell sorting efficiency (Table S3). In the same way, *P. salinarum* affiliated sequences represented close to all sequences in the *P. salinarum* phycosphere eucaryotic dataset (Table S3). However, because of the small amounts of DNA extracted and the sequencing depth in *P. salinarum* and *A. fusiformis* phycospheres fractions, we needed to adapt the normalization procedures for the bacterial and microeukaryotic datasets by investigating 2,360 and 101 sequences per sample for Bacteria and 2,097 and 196 for microeukaryotes, respectively, which allowed the collection of almost all diversity (Figure S3). When retaining 2,360 sequences per sample in the bacterial dataset, we excluded all *P. salinarum* phycosphere samples that contained mostly *P. salinarum* mitochondrion sequences, thus we decided to apply a complementary normalization threshold corresponding to 101 sequences per sample (Table S2). The same protocol was applied for the microeukaryotic dataset as the 2,097 sequences threshold

281 excluded all the *A. fusiformis* phycosphere samples, we decided to investigate the
282 microeukaryotic members of *A. fusiformis* phycosphere using a 196 sequences threshold.
283 Normalization thresholds retained for *Archaea* was 4,000 sequences per sample allowing to
284 capture most of the diversity present in the samples (Figure S3).

285 Last, as time necessary to process enough cell events by flow cytometry could affect
286 phycosphere microbial composition, we first compared microbial communities issued from
287 upstream and downstream controls. By computing Jaccard indices at the OTUs presence-
288 absence level, we showed that bacterial, microeukaryotic and archaeal communities are
289 highly similar in upstream and downstream control with stresses being respectively: 0.16,
290 0.21, 0.11, and supported by the ANOSIM (p-value 1.10^{-6}, Figure 2). The same patterns
291 were recorded at the OTUs abundance, using Bray-Curtis indexes, showing the proximity
292 of communities in upstream and downstream controls (Figure S4). The microbial
293 community composition evaluated at the phylum_class level was also highly similar
294 between upstream and downstream controls (Figure S5). Thus, the three days necessary to
295 sort *A. fusiformis* and *P. salinarum* with their respective phycosphere did not alter
296 microbial communities' composition, validating our method to explore the microbiomes
297 from the *A. fusiformis* and *P. salinarum* phycospheres.
298
299 **Community structure retrieved in *A. fusiformis* and *P. salinarum* phycosphere**
300 Cell-sorting based on the fluorescence and size properties of cell populations from the
301 different samples allowed to collect *A. fusiformis* individuals and their associated
302 phycosphere (27,172 events on average) and *P. salinarum* individuals and their
303 phycosphere (1,025,034 events on average) (Table S1, Figure S1 and S2). Since we could
304 not sample biological replicates at the different sampled depth because of field constraints,

we chose to analyze the phycosphere diversity by pooling all depths together in the abundance table. As expected, a dominance of ribosomal sequences affiliated to the targeted phytoplanktonic species either in the 16S or 18S rRNA genes datasets was observed (*i.e.*, the dominance of *A. fusiformis* 16S sequences in the bacterial 16S rRNA genes dataset of the *A. fusiformis* phycosphere and that of *P. salinarum* in the eukaryotic 18S rRNA genes dataset sequences of the *P. salinarum* phycosphere, Figure S6 and Table S3), confirming the successful enrichments of the target groups. The direct consequence of the presence of the target host sequences in the bacterial and eucaryotic datasets is the reduction of the apparent sequencing depth for these particular pools. Nevertheless, the *A. fusiformis* and *P. salinarum* OTUs were conserved, and the datasets were analyzed focusing on OTUs presence-absence patterns rather than classically the number of sequences. This allows to obtain a representative view of the diversity which is less biased by the over representation of the dominant taxon, and which can be compared between samples to give trends of microbial structure divergences. Since the archaeal dataset was free of host sequences and not impacted by the targeted photosynthetic microorganism, we could investigate archaeal OTUs presence-absence, abundance, and phylogeny in detail.

Based on flow cytometry cell-sorting, we showed that microbial OTUs composition from *A. fusiformis* and *P. salinarum* phycospheres were different, as illustrated on NMDS plots for bacterial, microeukaryotic and archaeal communities (based on OTUs presence-absence, Figure 2 and OTUs abundance, Figure S4) and by the presence of specific OTUs in each phycosphere (Figure S7). Moreover, phycospheric microbial composition is slightly different from the microbiome retrieved as free-living in the water column of Lake Dziani Dzaha as suggested by the NMDS plots (Figure 2 and Figure S4) and the composition in OTUs (Figure 3). This was further supported by the number of

329 specific free-living OTUs that represented 31.9, 36.8 and 26.6% of bacterial,
330 microeukaryotic and archaeal communities (Figure 4).

331 In more details, in the *A. fusiformis* phycosphere, bacterial communities were
332 mostly composed of cyanobacterial OTUs (all being affiliated to *A. fusiformis*) accounting
333 for 52.9 % of the 274 observed OTUs. Other OTUs were affiliated with Bacteroidia (mostly
334 Bacteroidales and Chitinophagales), Alphaproteobacteria (mainly Rhodobacterales) and
335 Dethiobacteria, accounting for 10.6, 8.8 and 7.3% of bacterial OTUs, respectively (Figure
336 3A). This pattern contrasted with the *P. salinarum* phycosphere (Figure 3A) in which
337 bacterial OTUs communities consisted mainly of Alphaproteobacteria (mainly
338 Rhodobacterales) accounting for 20.4% of OTUs, and of several phyla each representing
339 about 10% of bacterial OTUs (among 206 OTUs) including Cyanobacteria (all being
340 affiliated to the Arthrospira PCC-7345 genus), Actinobacteria (mainly Nitriliruptorales),
341 Bacteroidia (mostly Bacteroidales) and Gammaproteobacteria (mainly
342 Ectothiorhodospirilales). In contrast, the bacterial free-living microbiome was dominated
343 by OTUs affiliated with Actinobacteria, Alphaproteobacteria, Bacteroidia and
344 Dethiobacteria, each representing over 10% of the identified OTUs (Figure 3A).

345 The microeukaryotic composition retrieved in both phycospheres was mainly
346 represented by OTUs affiliated to the Picocystophyceae class, representing 44.4 and 62.5%
347 of OTUs in *A. fusiformis* and *P. salinarum* phycospheres, respectively (all being *P.*
348 *salinarum* OTUs) and by a Chlorophyceae class (Figure 3B). This latter Chlorophyceae
349 class contained 3 OTUs affiliated with the rare volvocalean green algal genus *Lobomonas*
350 and represented 31.1 and 27.5% of the microeukaryotic OTUs in *A. fusiformis* and *P.*
351 *salinarum* phycospheres, respectively. *A. fusiformis* was also associated with Bikosea and
352 Placididae classes: 11.1 and 6.7% of OTUs, respectively, that were less frequent in the *P.*

353 *salinarum* phycosphere, 2.5 and 2.5%, respectively (Figure 3B). On the other hand, the
354 free-living microbiome was mainly composed of the Picocystophyceae class (*i.e.*
355 *Picocystis*), Jakobea and Bikosea classes, representing 56.4, 16.4 and 14.5% of
356 microeukaryotic OTUs, respectively (Figure 3B).

357 Analyses of archaeal communities also showed contrasted patterns in
358 phycospheric communities between *A. fusiformis* and *P. salinarum*. This was particularly
359 true for Woesearchaeales (Woesearchaeia), enriched in the *P. salinarum* phycosphere (*i.e.*,
360 70.1% of archaeal OTUs in the *P. salinarum* phycosphere *versus* 51% in the*A. fusiformis*
361 phycosphere, Figure 3). Opposite composition patterns were reported for
362 Methanomicrobiales (Halobacteriota), Methanofastidiosales (Euryarchaeota) or
363 Thermoplasmata MBGD and DHVEG-1 (Thermoplasmatota) that were lower in the *P.*
364 *salinarum* phycosphere (8.4, 4.8 and 5.3% of OTUs, respectively) compared to the *A.*
365 *fusiformis* phycosphere (13.5, 5.75 and 12.5% of OTUs, respectively). The archaeal free-
366 living microbiome is mainly composed of Woesearchaeales, Thermoplasmata MBGD and
367 DHVEG-1, Methanomicrobiales and Methanofastidiosales (73.2, 6.9, 5.4 and 5.1% of
368 OTUs, respectively). Despite an apparently similar composition to that found in the *A.*
369 *fusiformis* and even more *P. salinarum* phycosphere microbiomes, the Jaccard matrices,
370 established on an OTUs presence-absence matrix, suggested that OTUs from the three
371 fractions were different (Figure 2). This was congruent with the occurrence of OTUs
372 reported on the archaeal phylogeny (Figure 5), based on 421bp positions, showing that
373 whatever their taxonomic affiliation, most archaeal OTUs were retrieved in the free-living
374 microbiome (185 over 196 archaeal OTUs) suggesting the ubiquity of archaea in the water
375 column. A total of 116 archaeal OTUs were retrieved in *A. fusiformis* phycosphere and 116
376 OTUs retrieved in the *P. salinarum* phycosphere. A focus on Woesearchaeales (129 OTUs

over 196 archaeal ones) highlighted that 125 OTUs were retrieved in the free-living microbiome, 60 in the *A. fusiformis* phycosphere and 76 in the *P. salinarum* phycosphere, and interestingly 47 woesearchaeal OTUs were retrieved in both phycospheres and free-living microbiomes (Figure 5). Noticeably, 43 woesearchaeal OTUs were specific to the free-living microbiome, many of which are phylogenetically close, while only 4 OTUs were specific to the phycospheres (*i.e.* particule-attached). The abundance of archaeal OTUs allowed the characterization of three contrasted profiles: First, OTUs for which the abundance in phycospheres was in the same range as that in the free-living microbiome, for example OTUs 2, 4, 13, 36, 148, 261, 138. Second, some OTUs that were less abundant in the free-living microbiome compared to the phycospheres, such as OTUs 558, 235 or 441. Finally, some OTUs that were more abundant in the free-living microbiome compared to the phycospheres, for example OTUs 10, 34, 47, 49, 57, 75, 91, 222, 202, 390 (Figure 5).

Discussion

We used flow cytometry cell-sorting to collect both *A. fusiformis* and *P. salinarum* cells in association with their surrounding associated phycospheres, offering the possibility to work at the microbial scale compared to previous studies which were performed at a larger scale. In fact, inherently to its functioning, flow cytometry isolates the objects to analyze, *e.g.* here the *Picocystis* or *Arthrospira* cells, in micro-droplets. By setting the sorting to favor unique events (one cell per droplet), we can isolate the cell with its closely associated surrounding water layer, *e.g.* its phycosphere. The size of the droplets used here, 60µm, is in adequation to theorical ranges of phycosphere radius calculated by Seymour and colleagues (2017).

Different composition of *A. fusiformis* and *P. salinarum* phycospheres

The present work showed different microbial compositions, at the OTUs level, between the *A. fusiformis* and *P. salinarum* phycospheres, with contrasted dominant OTUs being reported. Previous works, conducted on microorganisms associated with photosynthetic cells in marine ecosystems, reported mostly Rhodobacterales (*i.e.* Alphaproteobacteria), such as in the *P. salinarum* phycosphere, and Bacteroidia, such as in both *P. salinarum* and *A. fusiformis* phycospheres (Buchan et al., 2014; Teeling et al., 2012). The specificity of some associated bacterial members recovered here in the *A. fusiformis* and *P. salinarum* phycosphere microenvironments, such as Nitriliruptorales or Ectothiorhodospirilales is in agreement with the uniqueness of Lake Dziani Dzaha and the adapted communities retrieved in its water column (Hugoni et al., 2018). Moreover, the retrieval of eukaryotic members affiliated with Bikosea and Placididae, mainly from the *A. fusiformis* phycosphere, is consistent with their size, Bikosea being on average 3–4 µm wide and 5–6 µm length, (Jirsová et al., 2019) and Placididae, 3-10µm length and 2-7µm wide, (Rybarski et al., 2021), which are essentially larger than Picocystis. While being previously retrieved in hypersaline environments, the Bikosea ecology remains unclear (Jirsová et al., 2019; Park & Simpson, 2015). The presence of several Chlorophyceae OTUs affiliated with the *Lobomonas* genus in both phycospheres is highly interesting as we did not detect those OTUs in the large ecosystemic studies we previously performed (Bernard et al., 2019; Hugoni et al., 2018), suggesting that we missed those OTUs because of the large scale employed, proving further value to the microscaled studies as performed here.

Contrasted free-living microbiome compared to phycospheric microbiomes

Noticeably, our work highlighted that the free-living microbiome was different from the one retrieved from the phycospheres and did not reflect a possible leakage of the *A. fusiformis* or *P. salinarum* phycosphere microbiomes in the filtrate or a possible capture of microbial cells by the *A. fusiformis* or *P. salinarum* cells at the filtration step. This demonstrates our postulate that the microalgae *Picocystis* indeed harbors a phycosphere. We show here that this phycosphere microbiome is different from that of the *A. fusiformis* one. The proximity of the *P. salinarum* phycosphere microbiome and the free-living microbiome may have been enhanced in our study due to technical issues and may only partially represent the true *P. salinarum* phycosphere microbiome. Indeed, it is widely considered that the free-living microbiome is accessible through the classical differential filtering considering the 3 to 0.2 µm fraction. In consequence, we could not exclude that some *P. salinarum* small cells pass the 3µm filters and their phycosphere could be retrieved in the "free living" microbiome (3 to 0.2 µm fraction). The presence of small cells phycosphere is congruent with previous studies focusing on *Prochlorococcus* and *Synechococcus* (from 0.7 to 1.5 µm) reporting their physical associations with heterotrophic bacteria (Malfatti & Azam, 2009) and chemotaxis through their exudates (J. Seymour et al., 2010).

New insights into archaeal microbiomes in the phycosphere

The archaeal assemblage retrieved both at a large ecosystemic scale in the water column of Lake Dziani Dzaha and at a microscale in both phycospheres is largely dominated by OTUs affiliated with the Woesearchaeales. Woesearchaeales are members of the DPANN superphyla, which includes fast-evolving archaeal species (Adam et al., 2017; Dombrowski et al., 2020), that are diverse and broadly distributed in the biosphere. Few culturable

449 representatives of DPANN are available. Nevertheless, studies revealed that they presented
450 an extremely small cell size (0.1-0.8 µm; (Dombrowski et al., 2020)) and a reduced genome
451 (≈0.5 to 3 Mb, (Castelle et al., 2018)) associated with limited metabolic capabilities,
452 suggesting they may depend on symbiotic interactions with other organisms or may even
453 comprise novel parasitic species (Castelle et al., 2015; Dombrowski et al., 2019). While
454 numerous studies hypothesized an obligate symbiotic and/or parasitic lifestyle for DPANN
455 archaea (Golyshina et al., 2017; Hamm et al., 2019; Huber et al., 2002; Schwank et al.,
456 2019), a growing number of recent works suggested wider metabolic capabilities allowing a
457 free-living lifestyle in some DPANN members, such as Micrarchaeota (Kadnikov et al.,
458 2020) or "*Ca. Iainarchaeum andersonii"* affiliated with Diapherotrites (Youssef et al.,
459 2015). Here, we can hypothesize that, in Lake Dziani Dzaha, there are two kinds of
460 Woesearchaeales, (i) the ones that lives as particle-attached OTUs to a phytoplanktonic
461 species and (ii) the ones that lives as free-living (*i.e.* not as attached to phytoplankton:
462 fraction < 3µm) for which we could not exclude interactions with other small microbial
463 cells. While the Woesearchaeales metabolism remains unclear, a recent study of Lake A
464 (Canadian High Arctic lake), which presents extreme physico-chemical gradients and
465 sulfidic waters as observed in Lake Dziani Dzaha, detected sulfur/thiosulfate oxidation and
466 sulfite and sulfur reduction potentials in Woesearchaeota reconstructed genomes (Vigneron
467 et al., 2022). We suppose that in the water column conditions of Lake Dziani Dzaha, that
468 are organic-rich and where oxygen saturation decreases sharply from the surface to 5m
469 depth (from 180 to 2.7%) and becomes anoxic below, that free-living Woesearchaeales
470 might possess key metabolic pathways for heterotrophic autonomous growth such as
471 glycolysis, ATP generation or nucleotide biosynthesis. Thus, we hypothesize that, in this
472 anoxic zone, the ecological role of free-living Woesearchaeales might be the fermentation

of organic compounds that come from photosynthetic biomass degradation and which fermentation by-products will be further consumed by methanogenic Archaea, performing the final step of organic matter mineralization (Huang et al., 2021). In contrast, in the phycosphere, attached-Woesearchaeales might take direct advantage from low molecular compounds from photosynthetates exudated by their host cell, from transparent exopolymeric particles (TEP) and exopolymeric substances (EPS) (Christian & Anderson, 2002), and in turn ferment some of these compounds making their secondary metabolites accessible to the cells. Over time, Woesearchaeota that have benefited of key nutrients and cellular building blocks from their hosts might have adapted to these conditions by losing key pathways involved in their synthesis in central metabolism, as reported for DPANN archaea.

Among other archaeal classes retrieved in Lake Dziani Dzaha, most are methanogens and thus, strictly anaerobic. Their presence in the water column, even in layers where oxygen is still present suggested either a tolerance to oxygen exposure (Angel et al., 2011) and/or the presence of anoxic micro-niches in the *A. fusiformis* cells periphery and to a lesser extent in *P. salinarum* cells periphery, because of its lower size. High methane fluxes were observed in Lake Dziani Dzaha (Cadeau et al., 2020), that could not only depend on abiotic lithogenic inputs, and which could be the consequence of the "methane paradox" (unexplained accumulation of methane in oxic layers of aquatic ecosystems) (Günthel et al., 2019). Different mechanisms could explain this methane fluxes in Lake Dziani Dzaha. The first is based on the ability of different microorganisms to demethylate organic matter occurring when bacteria, including cyanobacteria, scavenge phosphorus, sulfur or nitrogen sources, cleave a methyl group to convert it in methane (Bizic, 2021). Second, regardless and independently of the presence of methylated

compounds in the water column, it has been shown that cyanobacteria could produce methane from CO_2 concomitantly with oxygen emission (Bižić et al., 2020). It has also been shown that the eukaryotic phytoplankton could also produce methane through different ways (Klintzsch et al., 2019). In classical aquatic ecosystems, in which cyanobacteria and eukaryotic green algae do not represent the vast majority of the biomass, photosynthesis-associated methane emissions might not be sufficient to account for a significant fraction of methanogenesis in comparison to methanogenic archaea (Bizic, 2021). However, in Lake Dziani Dzaha were *A. fusiformis* and *P. salinarum* account for almost 566 to 702 $\mu g.L^{-1}$ of chlorophyll *a* (Leboulanger et al., 2017), the photosynthesis-associated methane emissions might become significant to apprehend lake functioning.

Analogies with the terrestrial plant-root interface, *i.e.* the rhizosphere

While being a fundamental ecological interface, the phycosphere micro-environment has been paid much less attention compared to its terrestrial analogue, *i.e.* the rhizosphere. Here, we showed for the archaeal compartment, that most of the OTUs are widespread in the water column as free-living microorganisms and that several of them, being phylogenetically close, could also be retrieved in the phycosphere environment. This result suggested that phytoplanktonic species select specific archaeal OTUs, which sounded very similar to what is known as the rhizosphere effect, *i.e.*, the stimulation and selection of microbial communities by organic material exudated by plants in their rhizosphere, the recruitment of a root-adapted microbiome (Haichar et al., 2008; Uroz et al., 2019). In brief, our results confirm that the phycosphere is a dynamic microenvironment promoting microbial interactions, to which the ecological concepts described in the rhizosphere might be transposed.

Conclusions

Our work is the first to explore the microbial communities thriving in the phycosphere of bacterial (*A. fusiformis*), and eukaryotic (*P. salinarum*) phytoplanktonic populations by coupling flow-cytometry cell-sorting and metabarcoding of the three-domains-of-life. We took advantage of the comparison of microorganisms associated to the phycosphere *versus* free-living ones to identify contrasts in the microbiomes of the phycospheres and the water column. By investigating archaeal patterns, we showed that most of the Woesearchaeales from Lake Dziani Dzaha were preferentially free-living members and that the phytoplanktonic species promoted the selection of specific archaeal OTUs.

Further work will be needed to confirm this selection for bacteria and microeukaryotes, and a deeper investigation of the mechanisms involved in OTU selection will be necessary, in order to prove that a phycosphere effect exist (selection of specific OTUs through the interaction with phytoplanktonic species) and to identify the key metabolites involved in these interactions. However, the current study sets the stage for a better understanding of the relationships between microbials cells and how each and everyone, regardless of their size, can influence their (very) local environment.

Acknowledgments and funding sources

The authors wish to thank the Air Austral Airline Company, and Alexandra and Laurent at the “Les Couleurs” Guest House in Mayotte for their valuable assistance and support. This work was granted by a MITI CNRS “Défi Origines, de l’inerte au vivant” ORACLE (2018-2019) and a MITI CNRS « Défi X-life” CABMAN (2018-2019). We thank Marc Lacombe for his help on experimentations.

Conflict of interest statement

The authors declare that there is no conflict of interest.

Benefit-Sharing statement

The field permit was granted by the Conservatoire du Littoral et des Rivages Lacustres, Antenne Océan Indien, due to the fact that Lake Dziani Dzaha is currently a protected water body with free public access but restricted activities, under the control of the French agency for littoral ecosystems conservation (http://www.conservatoire-du-littoral.fr/).

Authors contribution

C.B, M.T, M.H designed research.

P.G, L.G, M.H, G.S, D.J performed research.

M.B, P.M.O, D.M, S.D, C.B, M.T, M.A, M.H, C.B, H.A, A.E analyze data.

L.A.C, M.B, M.H, prepared the figures.

M.B, P.M.O, D.M, S.D, C.B, M.T, M.A, M.H wrote the manuscript.

References

Adam, P. S., Borrel, G., Brochier-Armanet, C., & Gribaldo, S. (2017). The growing tree of Archaea: New perspectives on their diversity, evolution and ecology. *The ISME Journal*, *11*(11), 2407–2425. https://doi.org/10.1038/ismej.2017.122

Allison, S. D., & Martiny, J. B. H. (2008). Resistance, resilience, and redundancy in microbial communities. *Proceedings of the National Academy of Sciences of the United States of America*, *105*(Supplement 1), 11512–11519. https://doi.org/10.1073/pnas.0801925105

Amin, S. A., Green, D. H., Hart, M. C., Küpper, F. C., Sunda, W. G., & Carrano, C. J. (2009). Photolysis of iron–siderophore chelates promotes bacterial–algal mutualism. *Proceedings of the National Academy of Sciences of the United States of America*, *106*(40), 17071–17076. https://doi.org/10.1073/pnas.0905512106

Amin, S. A., Hmelo, L. R., van Tol, H. M., Durham, B. P., Carlson, L. T., Heal, K. R., Morales, R. L., Berthiaume, C. T., Parker, M. S., Djunaedi, B., Ingalls, A. E., Parsek, M. R., Moran, M. A., & Armbrust, E. V. (2015). Interaction and signalling between a cosmopolitan phytoplankton and associated bacteria. *Nature*, *522*(7554), Article 7554. https://doi.org/10.1038/nature14488

Angel, R., Matthies, D., & Conrad, R. (2011). Activation of methanogenesis in arid biological soil crusts despite the presence of oxygen. *PLoS One*, *6*(5), e20453. https://doi.org/10.1371/journal.pone.0020453

Ashraf, N., Ahmad, F., & Lu, Y. (2023). Synergy between microalgae and microbiome in polluted waters. *Trends in Microbiology*, *31*(1), 9–21. https://doi.org/10.1016/j.tim.2022.06.004

Bell, W., & Mitchell, R. (1972). Chemotactic and growth responses of marine bacteria to algal extracellular products. *The Biological Bulletin*, *143*(2), 265–277. https://doi.org/10.2307/1540052

Bernard, C., Escalas, A., Villeriot, N., Agogué, H., Hugoni, M., Duval, C., Carré, C., Got, P., Sarazin, G., Jézéquel, D., Leboulanger, C., Grossi, V., Ader, M., & Troussellier,

M. (2019). Very low phytoplankton diversity in a tropical saline-alkaline lake, with co-dominance of *Arthrospira fusiformis* (Cyanobacteria) and *Picocystis salinarum* (Chlorophyta). *Microbial Ecology*, *78*(3), Article 3. https://doi.org/10.1007/s00248-019-01332-8

Bizic, M. (2021). Phytoplankton photosynthesis: An unexplored source of biogenic methane emission from oxic environments. *Journal of Plankton Research*, fbab069. https://doi.org/10.1093/plankt/fbab069

Bižić, M., Klintzsch, T., Ionescu, D., Hindiyeh, M. Y., Günthel, M., Muro-Pastor, A. M., Eckert, W., Urich, T., Keppler, F., & Grossart, H.-P. (2020). Aquatic and terrestrial cyanobacteria produce methane. *Science Advances*, *6*(3), eaax5343. https://doi.org/10.1126/sciadv.aax5343

Bokulich, N. A., Subramanian, S., Faith, J. J., Gevers, D., Gordon, J. I., Knight, R., Mills, D. A., & Caporaso, J. G. (2013). Quality-filtering vastly improves diversity estimates from Illumina amplicon sequencing. *Nature Methods*, *10*(1), 57–59. https://doi.org/10.1038/nmeth.2276

Buchan, A., LeCleir, G. R., Gulvik, C. A., & González, J. M. (2014). Master recyclers: Features and functions of bacteria associated with phytoplankton blooms. *Nature Reviews Microbiology*, *12*(10), Article 10. https://doi.org/10.1038/nrmicro3326

Cadeau, P., Jezequel, D., Leboulanger, C., Fouilland, E., Le Floc'h, E., Chaduteau, C., Milesi, V., Guelard, J., Sarazin, G., Katz, A., d'Amore, S., Bernard, C., & Ader, M. (2020). New evidence that methane regulated early Earth's climate. *Scientific Reports*, *10*(18186), Article 18186. https://doi.org/10.1038/s41598-020-75100-x

612 Camacho, C., Coulouris, G., Avagyan, V., Ma, N., Papadopoulos, J., Bealer, K., &
613 Madden, T. L. (2009). BLAST+: Architecture and applications. *BMC*
614 *Bioinformatics*, *10*, 421. https://doi.org/10.1186/1471-2105-10-421
615 Caporaso, J. G., Lauber, C. L., Walters, W. A., Berg-Lyons, D., Lozupone, C. A.,
616 Turnbaugh, P. J., Fierer, N., & Knight, R. (2011). Global patterns of 16S rRNA
617 diversity at a depth of millions of sequences per sample. *Proceedings of the*
618 *National Academy of Sciences of the United States of America*, *108*(Suppl 1), 4516–
619 4522. https://doi.org/10.1073/pnas.1000080107
620 Castelle, C. J., Brown, C. T., Anantharaman, K., Probst, A. J., Huang, R. H., & Banfield, J.
621 F. (2018). Biosynthetic capacity, metabolic variety and unusual biology in the CPR
622 and DPANN radiations. *Nature Reviews Microbiology*, *16*(10), 629–645.
623 https://doi.org/10.1038/s41579-018-0076-2
624 Castelle, C. J., Wrighton, K. C., Thomas, B. C., Hug, L. A., Brown, C. T., Wilkins, M. J.,
625 Frischkorn, K. R., Tringe, S. G., Singh, A., Markillie, L. M., Taylor, R. C.,
626 Williams, K. H., & Banfield, J. F. (2015). Genomic expansion of domain archaea
627 highlights roles for organisms from new phyla in anaerobic carbon cycling. *Current*
628 *Biology*, *25*(6), 690–701. https://doi.org/10.1016/j.cub.2015.01.014
629 Castresana, J. (2000). Selection of conserved blocks from multiple alignments for their use
630 in phylogenetic analysis. *Molecular Biology and Evolution*, *17*(4), 540–552.
631 https://doi.org/10.1093/oxfordjournals.molbev.a026334
632 Cellamare, M., Duval, C., Drelin, Y., Djediat, C., Touibi, N., Agogué, H., Leboulanger, C.,
633 Ader, M., & Bernard, C. (2018). Characterization of phototrophic microorganisms
634 and description of new cyanobacteria isolated from the saline-alkaline crater-lake

Dziani Dzaha (Mayotte, Indian Ocean). *FEMS Microbiology Ecology*, *94*(8). https://doi.org/10.1093/femsec/fiy108

Christian, J. R., & Anderson, T. R. (2002). Chapter 16—Modeling DOM Biogeochemistry. In D. A. Hansell & C. A. Carlson (Eds.), *Biogeochemistry of Marine Dissolved Organic Matter* (pp. 717–755). Academic Press. https://doi.org/10.1016/B978-012323841-2/50018-X

Cordero, O. X., & Datta, M. S. (2016). Microbial interactions and community assembly at microscales. *Current Opinion in Microbiology*, *31*, 227–234. https://doi.org/10.1016/j.mib.2016.03.015

Croft, M. T., Lawrence, A. D., Raux-Deery, E., Warren, M. J., & Smith, A. G. (2005). Algae acquire vitamin B12 through a symbiotic relationship with bacteria. *Nature*, *438*(7064), Article 7064. https://doi.org/10.1038/nature04056

Dadheech, P. K., Glöckner, G., Casper, P., Kotut, K., Mazzoni, C. J., Mbedi, S., & Krienitz, L. (2013). Cyanobacterial diversity in the hot spring, pelagic and benthic habitats of a tropical soda lake. *FEMS Microbiology Ecology*, *85*(2), 389–401. https://doi.org/10.1111/1574-6941.12128

Dal Co, A., van Vliet, S., Kiviet, D. J., Schlegel, S., & Ackermann, M. (2020). Short-range interactions govern the dynamics and functions of microbial communities. *Nature Ecology & Evolution*, *4*(3), Article 3. https://doi.org/10.1038/s41559-019-1080-2

Dombrowski, N., Lee, J.-H., Williams, T. A., Offre, P., & Spang, A. (2019). Genomic diversity, lifestyles and evolutionary origins of DPANN archaea. *FEMS Microbiology Letters*, *366*(2). https://doi.org/10.1093/femsle/fnz008

Dombrowski, N., Williams, T. A., Sun, J., Woodcroft, B. J., Lee, J.-H., Minh, B. Q., Rinke, C., & Spang, A. (2020). Undinarchaeota illuminate DPANN phylogeny and the

impact of gene transfer on archaeal evolution. *Nature Communications*, *11*(1), Article 1. https://doi.org/10.1038/s41467-020-17408-w

Escalas, A., Troussellier, M., Melayah, D., Bruto, M., Nicolas, S., Bernard, C., Ader, M., Leboulanger, C., Agogué, H., & Hugoni, M. (2021). Strong reorganization of multi-domain microbial networks associated with primary producers sedimentation from oxic to anoxic conditions in an hypersaline lake. *FEMS Microbiology Ecology*, *97*(12), fiab163. https://doi.org/10.1093/femsec/fiab163

Escudié, F., Auer, L., Bernard, M., Mariadassou, M., Cauquil, L., Vidal, K., Maman, S., Hernandez-Raquet, G., Combes, S., & Pascal, G. (2017). FROGS: Find, Rapidly, OTUs with Galaxy Solution. *Bioinformatics*, *34*(8), 1287–1294. https://doi.org/10.1093/bioinformatics/btx791

Fu, H., Uchimiya, M., Gore, J., & Moran, M. A. (2020). Ecological drivers of bacterial community assembly in synthetic phycospheres. *Proceedings of the National Academy of Sciences of the United States of America*, *117*(7), Article 7. https://doi.org/10.1073/pnas.1917265117

Golyshina, O. V., Toshchakov, S. V., Makarova, K. S., Gavrilov, S. N., Korzhenkov, A. A., La Cono, V., Arcadi, E., Nechitaylo, T. Y., Ferrer, M., Kublanov, I. V., Wolf, Y. I., Yakimov, M. M., & Golyshin, P. N. (2017). "ARMAN" archaea depend on association with euryarchaeal host in culture and in situ. *Nature Communications*, *8*(1), 60. https://doi.org/10.1038/s41467-017-00104-7

Günthel, M., Donis, D., Kirillin, G., Ionescu, D., Bizic, M., McGinnis, D. F., Grossart, H.-P., & Tang, K. W. (2019). Contribution of oxic methane production to surface methane emission in lakes and its global importance. *Nature Communications*, *10*(1), Article 1. https://doi.org/10.1038/s41467-019-13320-0

683 Haichar, F. el Z., Marol, C., Berge, O., Rangel-Castro, J. I., Prosser, J. I., Balesdent, J.,
684 Heulin, T., & Achouak, W. (2008). Plant host habitat and root exudates shape soil
685 bacterial community structure. *The ISME Journal*, *2*(12), Article 12.
686 https://doi.org/10.1038/ismej.2008.80
687 Halary, S., Duperron, S., Demay, J., Duval, C., Hamlaoui, S., Piquet, B., Reinhardt, A.,
688 Bernard, C., & Marie, B. (2022). Metagenome-based exploration of bacterial
689 communities associated with Cyanobacteria strains isolated from thermal muds.
690 *Microorganisms*, *10*(12), 2337. https://doi.org/10.3390/microorganisms10122337
691 Hamm, J. N., Erdmann, S., Eloe-Fadrosh, E. A., Angeloni, A., Zhong, L., Brownlee, C.,
692 Williams, T. J., Barton, K., Carswell, S., Smith, M. A., Brazendale, S., Hancock, A.
693 M., Allen, M. A., Raftery, M. J., & Cavicchioli, R. (2019). Unexpected host
694 dependency of Antarctic Nanohaloarchaeota. *Proceedings of the National Academy*
695 *of Sciences of the United States of America*, *116*(29), 14661–14670.
696 https://doi.org/10.1073/pnas.1905179116
697 Huang, W. C., Liu, Y., Zhang, X., Zhang, C. J., Zou, D., Zheng, S., Xu, W., Luo, Z., Liu,
698 F., Li, M. (2021) Comparative genomic analysis reveals metabolic flexibility of
699 Woesearchaeota. *Nature Communications*, *12*, 5281.
700 https://doi.org/10.1038/s41467-021-25565-9
701 Huber, H., Hohn, M. J., Rachel, R., Fuchs, T., Wimmer, V. C., & Stetter, K. O. (2002). A
702 new phylum of Archaea represented by a nanosized hyperthermophilic symbiont.
703 *Nature*, *417*(6884), Article 6884. https://doi.org/10.1038/417063a
704 Hugoni, M., Domaizon, I., Taib, N., Biderre-Petit, C., Agogué, H., Galand, P. E., Debroas,
705 D., & Mary, I. (2015). Temporal dynamics of active Archaea in oxygen-depleted

zones of two deep lakes. *Environmental Microbiology Reports*, *7*(2), Article 2. https://doi.org/10.1111/1758-2229.12251

Hugoni, M., Escalas, A., Bernard, C., Nicolas, S., Jézéquel, D., Vazzoler, F., Sarazin, G., Leboulanger, C., Bouvy, M., Got, P., Ader, M., Troussellier, M., & Agogué, H. (2018). Spatiotemporal variations in microbial diversity across the three domains of life in a tropical thalassohaline lake (Dziani Dzaha, Mayotte Island). *Molecular Ecology*, *27*, 4775–4786.

Jirsová, D., Füssy, Z., Richtová, J., Gruber, A., & Oborník, M. (2019). Morphology, ultrastructure, and mitochondrial genome of the marine non-photosynthetic Bicosoecid Cafileria marina gen. Et sp. Nov. *Microorganisms*, *7*(8), Article 8. https://doi.org/10.3390/microorganisms7080240

Kadnikov, V. V., Savvichev, A. S., Mardanov, A. V., Beletsky, A. V., Chupakov, A. V., Kokryatskaya, N. M., Pimenov, N. V., & Ravin, N. V. (2020). Metabolic diversity and evolutionary history of the archaeal phylum "Candidatus *Micrarchaeota*" uncovered from a freshwater lake metagenome. *Applied and Environmental Microbiology*, *86*(23). https://doi.org/10.1128/AEM.02199-20

Klintzsch, T., Langer, G., Nehrke, G., Wieland, A., Lenhart, K., & Keppler, F. (2019). Methane production by three widespread marine phytoplankton species: Release rates, precursor compounds, and potential relevance for the environment. *Biogeosciences*, *16*(20), 4129–4144. https://doi.org/10.5194/bg-16-4129-2019

Krienitz, L., Dadheech, P. K., & Kotut, K. (2013). Mass developments of the cyanobacteria Anabaenopsis and Cyanospira (Nostocales) in the soda lakes of Kenya: Ecological and systematic implications. *Hydrobiologia*, *703*(1), 79–93. https://doi.org/10.1007/s10750-012-1346-z

Kuraku, S., Zmasek, C. M., Nishimura, O., & Katoh, K. (2013). ALeaves facilitates on-demand exploration of metazoan gene family trees on MAFFT sequence alignment server with enhanced interactivity. *Nucleic Acids Research*, *41*(Web Server issue), W22-28. https://doi.org/10.1093/nar/gkt389

Leboulanger, C., Agogué, H., Bernard, C., Bouvy, M., Carré, C., Cellamare, M., Duval, C., Fouilland, E., Got, P., Intertaglia, L., Lavergne, C., Le Floc'h, E., Roques, C., & Sarazin, G. (2017). Microbial diversity and cyanobacterial production in Dziani Dzaha crater lake, a unique tropical thalassohaline environment. *PloS One*, *12*(1), e0168879. https://doi.org/10.1371/journal.pone.0168879

Lefort, V., Desper, R., & Gascuel, O. (2015). FastME 2.0: A Comprehensive, accurate, and fast distance-based phylogeny inference program: Table 1. *Molecular Biology and Evolution*, *32*(10), 2798–2800. https://doi.org/10.1093/molbev/msv150

Lepère, C., Domaizon, I., Hugoni, M., Vellet, A., & Debroas, D. (2016). Diversity and dynamics of active small microbial eukaryotes in the anoxic zone of a freshwater meromictic lake (Pavin, France). *Frontiers in Microbiology*, *7*, 130. https://doi.org/10.3389/fmicb.2016.00130

Li, J., Gu, L., Bai, S., Wang, J., Su, L., Wei, B., Zhang, L., & Fang, J. (2021). Characterization of particle-associated and free-living bacterial and archaeal communities along the water columns of the South China Sea. *Biogeosciences*, *18*(1), 113–133. https://doi.org/10.5194/bg-18-113-2021

Liu, J., Meng, Z., Liu, X., & Zhang, X.-H. (2019). Microbial assembly, interaction, functioning, activity and diversification: A review derived from community compositional data. *Marine Life Science & Technology*, *1*(1), 112–128. https://doi.org/10.1007/s42995-019-00004-3

Louati, I., Nunan, N., Tambosco, K., Bernard, C., Humbert, J.-F., & Leloup, J. (2023). The phyto-bacterioplankton couple in a shallow freshwater ecosystem: Who leads the dance? *Harmful Algae, 126*, 102436. https://doi.org/10.1016/j.hal.2023.102436

Mahé, F., Rognes, T., Quince, C., Vargas, C. de, & Dunthorn, M. (2014). Swarm: Robust and fast clustering method for amplicon-based studies. *PeerJ*, *2*, e593.

Malfatti, F., & Azam, F. (2009). Atomic force microscopy reveals microscale networks and possible symbioses among pelagic marine bacteria. *Aquatic Microbial Ecology*, *58*, 1–14. https://doi.org/10.3354/ame01355

Orland, C., Yakimovich, K. M., Mykytczuk, N. C. S., Basiliko, N., & Tanentzap, A. J. (2020). Think global, act local: The small-scale environment mainly influences microbial community development and function in lake sediment. *Limnology and Oceanography*, *65*(S1), S88–S100. https://doi.org/10.1002/lno.11370

Pálmai, T., Szabó, B., Kotut, K., Krienitz, L., & Padisák, J. (2020). Ecophysiology of a successful phytoplankton competitor in the African flamingo lakes: The green alga *Picocystis salinarum* (Picocystophyceae). *Journal of Applied Phycology*, *32*(3), 1813–1825. https://doi.org/10.1007/s10811-020-02092-6

Park, J. S., & Simpson, A. G. B. (2015). Diversity of Heterotrophic Protists from Extremely Hypersaline Habitats. *Protist*, *166*(4), Article 4. https://doi.org/10.1016/j.protis.2015.06.001

Pascault, N., Rué, O., Loux, V., Pédron, J., Martin, V., Tambosco, J., Bernard, C., Humbert, J., & Leloup, J. (2021). Insights into the cyanosphere: Capturing the respective metabolisms of cyanobacteria and chemotrophic bacteria in natural conditions? *Environmental Microbiology Reports*, *13*(3), 364–374. https://doi.org/10.1111/1758-2229.12944

778 Pruesse, E., Quast, C., Knittel, K., Fuchs, B. M., Ludwig, W., Peplies, J., & Glöckner, F. O.
779 (2007). SILVA: A comprehensive online resource for quality checked and aligned
780 ribosomal RNA sequence data compatible with ARB. *Nucleic Acids Research*,
781 *35*(21), 7188–7196. https://doi.org/10.1093/nar/gkm864
782 Ramette, A. (2007). Multivariate analyses in microbial ecology. *FEMS Microbiology*
783 *Ecology*, *62*(2), Article 2. https://doi.org/10.1111/j.1574-6941.2007.00375.x
784 Ritchie, R. J. (2006). Consistent sets of spectrophotometric chlorophyll equations for
785 acetone, methanol and ethanol solvents. *Photosynthesis Research*, *89*(1), 27–41.
786 https://doi.org/10.1007/s11120-006-9065-9
787 Roesler, C. (2002). Distribution, production, and ecophysiology of Picocystis strain ML in
788 Mono Lake, California. *Limnology and Oceanography*, *47*(2), 440–452.
789 Rognes, T., Flouri, T., Nichols, B., Quince, C., & Mahé, F. (2016). VSEARCH: A versatile
790 open source tool for metagenomics. *PeerJ*, *4*, e2584.
791 https://doi.org/10.7717/peerj.2584
792 Rybarski, A. E., Nitsche, F., Soo Park, J., Filz, P., Schmidt, P., Kondo, R., GB Simpson,
793 A., & Arndt, H. (2021). Revision of the phylogeny of Placididea (Stramenopiles):
794 Molecular and morphological diversity of novel placidid protists from extreme
795 aquatic environments. *European Journal of Protistology*, *81*, 125809.
796 https://doi.org/10.1016/j.ejop.2021.125809
797 Sapp, M., Schwaderer, A. S., Wiltshire, K. H., Hoppe, H.-G., Gerdts, G., & Wichels, A.
798 (2007). Species-specific bacterial communities in the phycosphere of microalgae?
799 *Microbial Ecology*, *53*(4), 683–699. https://doi.org/10.1007/s00248-006-9162-5
800 Sarazin, G., Jézéquel, D., Leboulanger, C., Fouilland, E., Floc'h, E. L., Bouvy, M., Gérard,
801 E., Agogué, H., Bernard, C., Hugoni, M., Grossi, V., Troussellier, M., & Ader, M.

(2021). Geochemistry of an endorheic thalassohaline ecosystem: The Dziani Dzaha crater lake (Mayotte Archipelago, Indian Ocean). *Comptes Rendus. Géoscience*, *0*(0), 1–19. https://doi.org/10.5802/crgeos.43

Schuurman, T., de Boer, R. F., Kooistra-Smid, A. M. D., & van Zwet, A. A. (2004). Prospective study of use of PCR amplification and sequencing of 16S ribosomal DNA from cerebrospinal fluid for diagnosis of bacterial meningitis in a clinical setting. *Journal of Clinical Microbiology*, *42*(2), 734–740. https://doi.org/10.1128/JCM.42.2.734-740.2004

Schwank, K., Bornemann, T. L. V., Dombrowski, N., Spang, A., Banfield, J. F., & Probst, A. J. (2019). An archaeal symbiont-host association from the deep terrestrial subsurface. *The ISME Journal*, *13*(8), 2135–2139. https://doi.org/10.1038/s41396-019-0421-0

Seyedsayamdost, M. R., Wang, R., Kolter, R., & Clardy, J. (2014). Hybrid biosynthesis of roseobacticides from algal and bacterial precursor molecules. *Journal of the American Chemical Society*, *136*(43), 15150–15153. https://doi.org/10.1021/ja508782y

Seymour, J., Ahmed, T., Durham, W., & Stocker, R. (2010). Chemotactic response of marine bacteria to the extracellular products of *Synechococcus* and *Prochlorococcus*. *Aquatic Microbial Ecology*, *59*, 161–168. https://doi.org/10.3354/ame01400

Seymour, J. R., Amin, S. A., Raina, J.-B., & Stocker, R. (2017). Zooming in on the phycosphere: The ecological interface for phytoplankton–bacteria relationships. *Nature Microbiology*, *2*(7), 17065. https://doi.org/10.1038/nmicrobiol.2017.65

Shibl, A. A., Isaac, A., Ochsenkühn, M. A., Cárdenas, A., Fei, C., Behringer, G., Arnoux, M., Drou, N., Santos, M. P., Gunsalus, K. C., Voolstra, C. R., & Amin, S. A. (2020). Diatom modulation of select bacteria through use of two unique secondary metabolites. *Proceedings of the National Academy of Sciences of the United States of America*, *117*(44), 27445–27455. https://doi.org/10.1073/pnas.2012088117

Sorokin, D. Y., Berben, T., Melton, E. D., Overmars, L., Vavourakis, C. D., & Muyzer, G. (2014). Microbial diversity and biogeochemical cycling in soda lakes. *Extremophiles*, *18*(5), 791–809. https://doi.org/10.1007/s00792-014-0670-9

Suzuki, A., Kaneko, R., Kodama, T., Hashihama, F., Suwa, S., Tanita, I., et al. (2017). Comparison of community structures between particle-associated and free-living prokaryotes in tropical and subtropical Pacific Ocean surface waters. *J. Oceanogr.* 73, 383–395. doi: 10.1007/s10872-016-0410-0

Talavera, G., & Castresana, J. (2007). Improvement of phylogenies after removing divergent and ambiguously aligned blocks from protein sequence alignments. *Systematic Biology*, *56*(4), 564–577. https://doi.org/10.1080/10635150701472164

Teeling, H., Fuchs, B. M., Becher, D., Klockow, C., Gardebrecht, A., Bennke, C. M., Kassabgy, M., Huang, S., Mann, A. J., Waldmann, J., Weber, M., Klindworth, A., Otto, A., Lange, J., Bernhardt, J., Reinsch, C., Hecker, M., Peplies, J., Bockelmann, F. D., … Amann, R. (2012). Substrate-controlled succession of marine bacterioplankton populations induced by a phytoplankton bloom. *Science (New York, N.Y.)*, *336*(6081), 608–611. https://doi.org/10.1126/science.1218344

Uroz, S., Courty, P. E., & Oger, P. (2019). Plant symbionts are engineers of the plant-associated microbiome. *Trends in Plant Science*, *24*(10), 905–916. https://doi.org/10.1016/j.tplants.2019.06.008

Vigneron, A., Cruaud, P., Lovejoy, C., & Vincent, W. F. (2022). Genomic evidence of functional diversity in DPANN archaea, from oxic species to anoxic vampiristic consortia. *ISME Communications*, *2*(1), 4. https://doi.org/10.1038/s43705-022-00088-6

Walters, W., Hyde, E. R., Berg-Lyons, D., Ackermann, G., Humphrey, G., Parada, A., Gilbert, J. A., Jansson, J. K., Caporaso, J. G., Fuhrman, J. A., Apprill, A., & Knight, R. (2016). Improved bacterial 16S rRNA gene (V4 and V4-5) and fungal internal transcribed spacer marker gene primers for microbial community surveys. *mSystems*, *1*(1), e00009-15. https://doi.org/10.1128/mSystems.00009-15

Wang, Q., Garrity, G. M., Tiedje, J. M., & Cole, J. R. (2007). Naive Bayesian classifier for rapid assignment of rRNA sequences into the new bacterial taxonomy. *Applied and Environmental Microbiology*, *73*(16), 5261–5267. https://doi.org/10.1128/AEM.00062-07

Woodhouse, J. N., Kinsela, A. S., Collins, R. N., Bowling, L. C., Honeyman, G. L., Holliday, J. K., & Neilan, B. A. (2016). Microbial communities reflect temporal changes in cyanobacterial composition in a shallow ephemeral freshwater lake. *The ISME Journal*, *10*(6), 1337–1351. https://doi.org/10.1038/ismej.2015.218

Yang, C., Wang, Q., Simon, P. N., Liu, J., Liu, L., Dai, X., Zhang, X., Kuang, J., Igarashi, Y., Pan, X., & Luo, F. (2017). Distinct network interactions in particle-associated and free-living bacterial communities during a *Microcystis aeruginosa* bloom in a plateau lake. *Frontiers in Microbiology*, *8*, 1202. https://doi.org/10.3389/fmicb.2017.01202

Youssef, N. H., Rinke, C., Stepanauskas, R., Farag, I., Woyke, T., & Elshahed, M. S. (2015). Insights into the metabolism, lifestyle and putative evolutionary history of

the novel archaeal phylum ‘Diapherotrites.’ *The ISME Journal*, *9*(2), Article 2. https://doi.org/10.1038/ismej.2014.141

Zhang, W., Ding, W., Li, Y.-X., Tam, C., Bougouffa, S., Wang, R., Pei, B., Chiang, H., Leung, P., Lu, Y., Sun, J., Fu, H., Bajic, V. B., Liu, H., Webster, N. S., & Qian, P.-Y. (2019). Marine biofilms constitute a bank of hidden microbial diversity and functional potential. *Nature Communications*, *10*(1), 517. https://doi.org/10.1038/s41467-019-08463-z

Zhou, J., Chen, G.-F., Ying, K.-Z., Jin, H., Song, J.-T., & Cai, Z.-H. (2019). Phycosphere Microbial Succession Patterns and Assembly Mechanisms in a Marine Dinoflagellate Bloom. *Applied and Environmental Microbiology*, *85*(15). https://doi.org/10.1128/AEM.00349-19

Data accessibility statement

The sequence data generated in this study were deposited in the EBI-ENA public database under the following accession number PRJEB60179, PRJEB60179, PRJEB42914, PRJEB42913 for microeukaryotes, bacteria and archaea, respectively.

Figures and tables

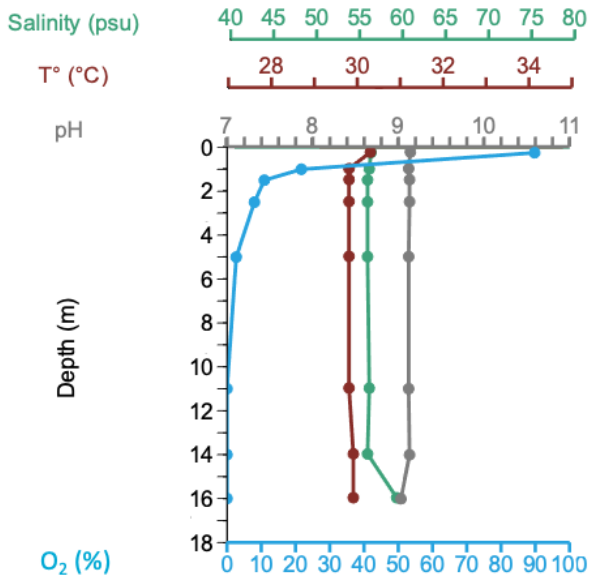

Figure 1. Vertical profiles of environmental parameters recorded along the water column. Salinity (psu), temperature (°C), pH, and O_2 saturation (%) profiles were recorded during November 2018.

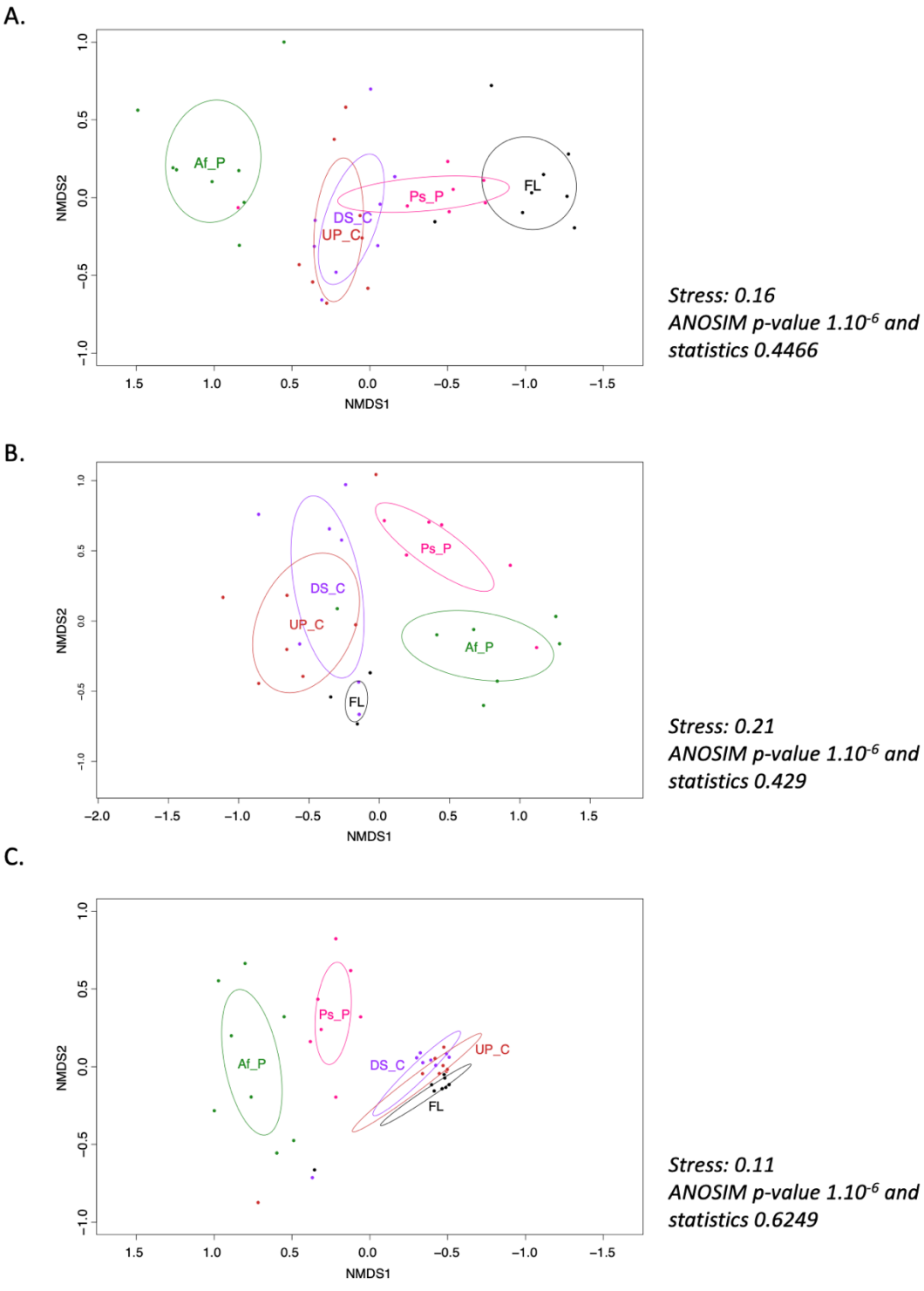

907

908 **Figure 2. Differences in (A) bacterial, (B) microeukaryotic and (C) archaeal**
909 **communities' structure, evaluated at the OTUs level.** NMDS ordination was performed
910 on Jaccard matrices based on presence-absence data. Jaccard indices were compiled

911 considering upstream (UP_C) and downstream controls (DS_C), *A. fusiformis* (Af_P) and
912 *P. salinarum* (Ps_P) phycospheres and the free-living (FL) microbiome (eight samples per
913 condition). To fully compare the OTUs composition in each condition, indices were
914 computed from the bacterial dataset normalized to 101 sequences, the microeukaryotic
915 dataset normalized to 196 sequences and the 4,000 sequences archaeal dataset.

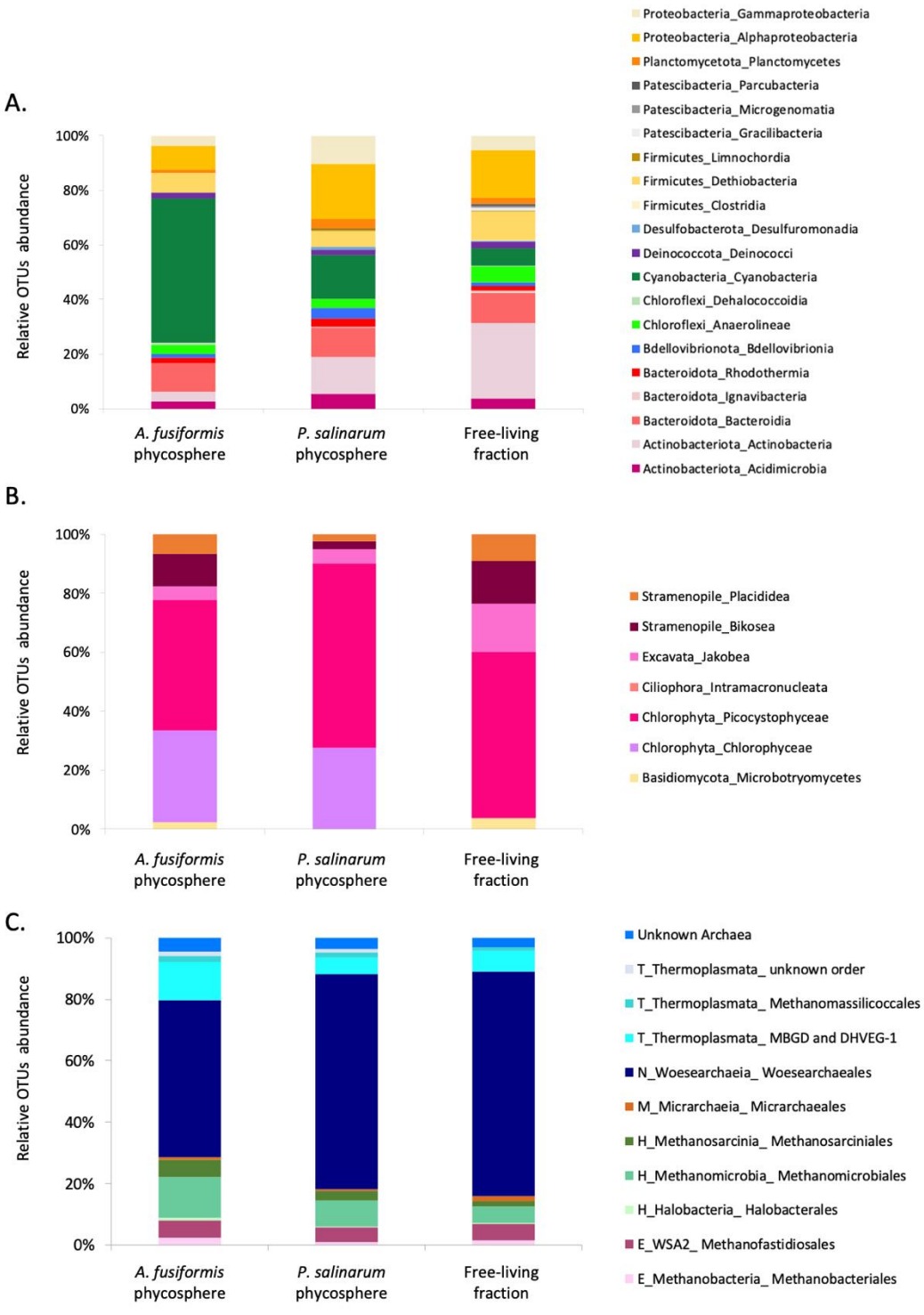
A.
Relative OTUs abundance
100%
80%
60%
40%
20%
0%
A. fusiformis phycosphere
P. salinarum phycosphere
Free-living fraction
Proteobacteria_Gammaproteobacteria
Proteobacteria_Alphaproteobacteria
Planctomycetota_Planctomycetes
Patescibacteria_Parcubacteria
Patescibacteria_Microgenomatia
Patescibacteria_Gracilibacteria
Firmicutes_Limnochordia
Firmicutes_Dethiobacteria
Firmicutes_Clostridia
Desulfobacterota_Desulfuromonadia
Deinococcota_Deinococci
Cyanobacteria_Cyanobacteria
Chloroflexi_Dehalococcoidia
Chloroflexi_Anaerolineae
Bdellovibrionota_Bdellovibrionia
Bacteroidota_Rhodothermia
Bacteroidota_Ignavibacteria
Bacteroidota_Bacteroidia
Actinobacteriota_Actinobacteria
Actinobacteriota_Acidimicrobia
B.
Relative OTUs abundance
100%
80%
60%
40%
20%
0%
A. fusiformis phycosphere
P. salinarum phycosphere
Free-living fraction
Stramenopile_Placididea
Stramenopile_Bikosea
Excavata_Jakobea
Ciliophora_Intramacronucleata
Chlorophyta_Picocystophyceae
Chlorophyta_Chlorophyceae
Basidiomycota_Microbotryomycetes
C.
Relative OTUs abundance
100%
80%
60%
40%
20%
0%
A. fusiformis phycosphere
P. salinarum phycosphere
Free-living fraction
Unknown Archaea
T_Thermoplasmata_ unknown order
T_Thermoplasmata_ Methanomassiliicoccales
T_Thermoplasmata_ MBGD and DHVEG-1
N_Woesearchaeia_ Woesearchaeales
M_Micrarchaeia_ Micrarchaeales
H_Methanosarcinia_ Methanosarciniales
H_Methanomicrobia_ Methanomicrobiales
H_Halobacteria_ Halobacterales
E_WSA2_ Methanofastidiosales
E_Methanobacteria_ Methanobacteriales

916

Figure 3. Relative OTUs abundance in *A. fusiformis* and *P. salinarum* phycospheres compared to free-living microbiome. Relative abundance of OTUs were declined for bacteria (A), microeukaryotes (B) and archaea (C).

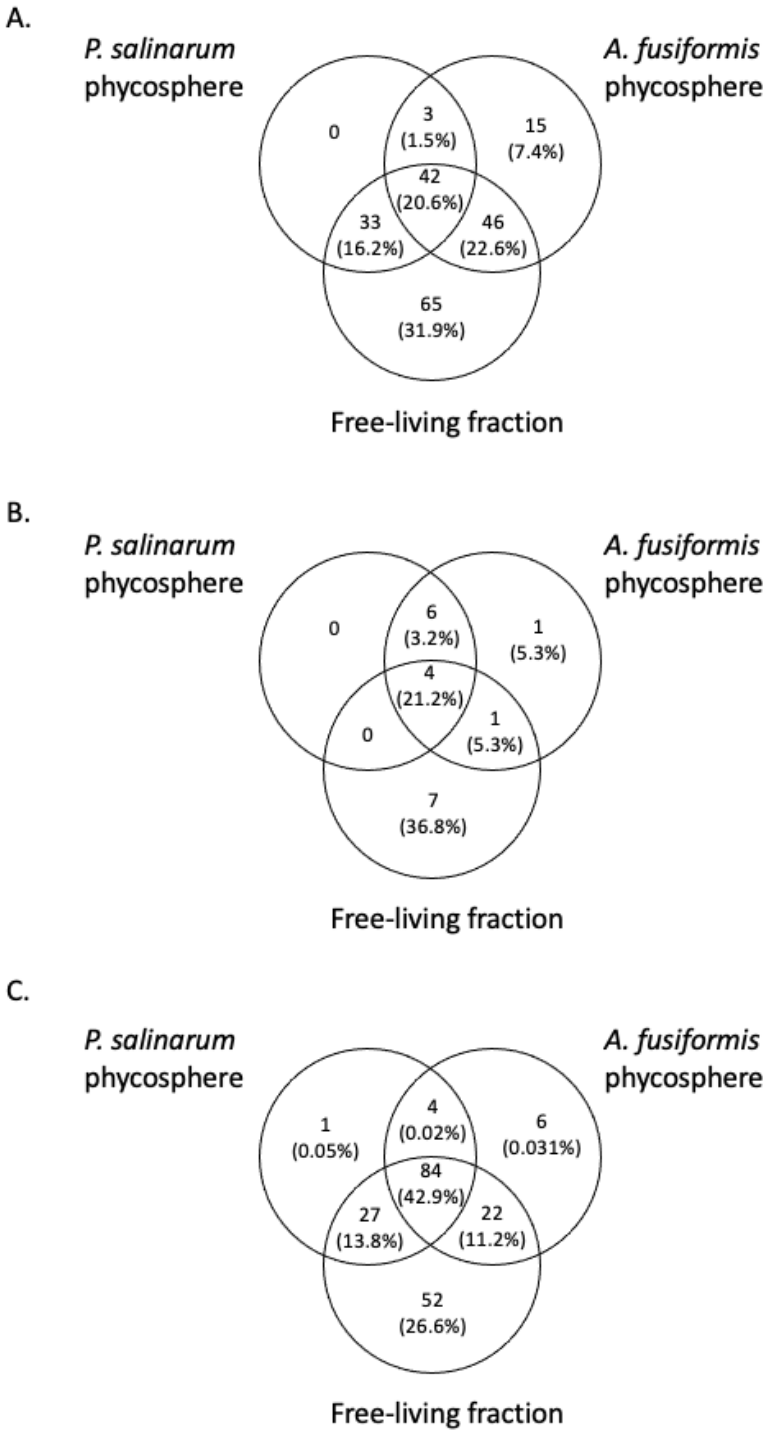

Figure 4. Distribution of OTUs among the *A. fusiformis* and *P. salinarum* phycospheres, and the free-living microbiome. Venn diagrams presenting shared and specific bacterial (A), microeukaryotic (B) and archaeal (C) OTUs.

A.

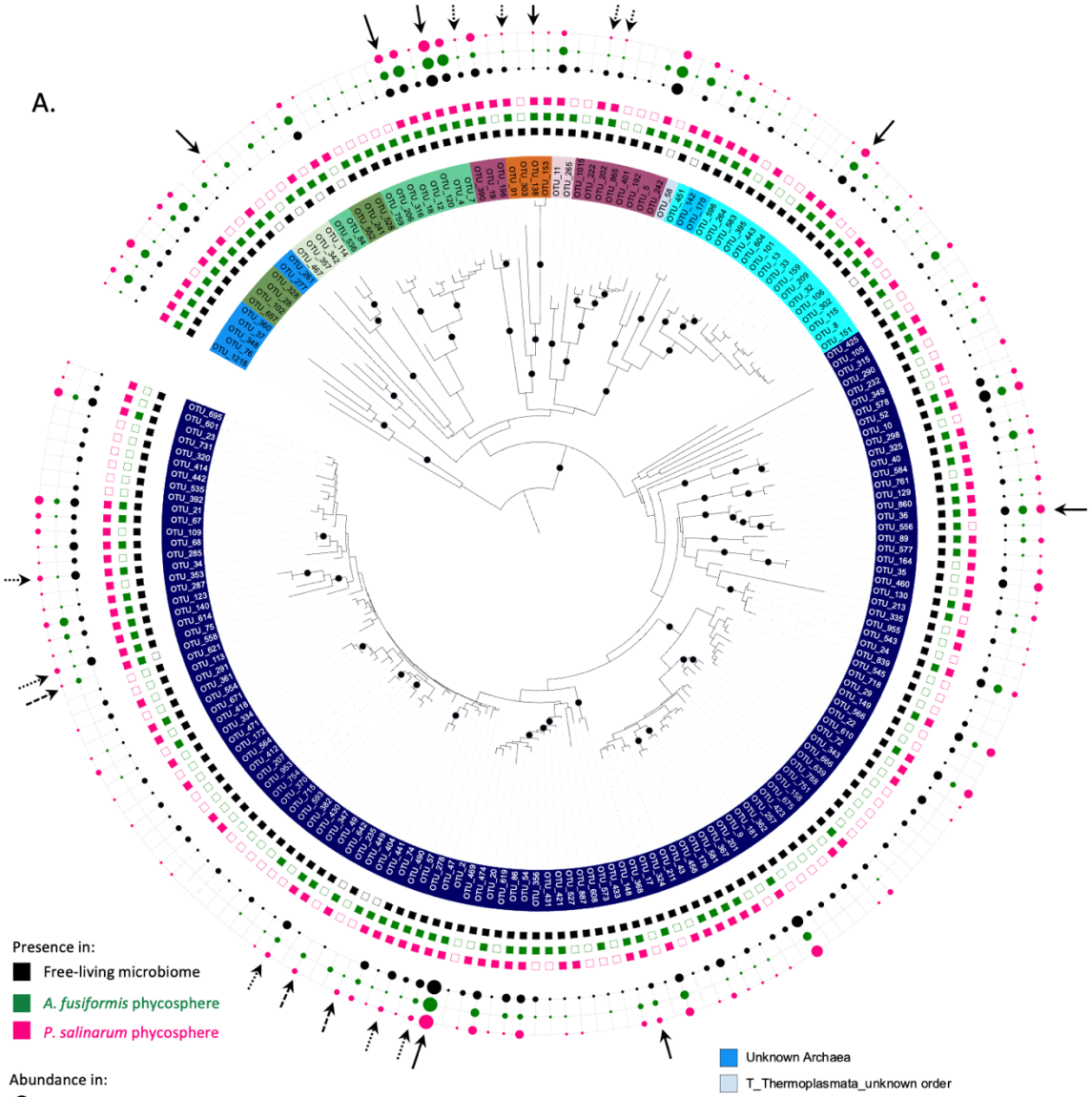

B.

	All	Common	Specific *A. fusiformis* phycosphere	Specific *P. salinarum* phycosphere	Specific Free-living fraction	Common *A. fusiformis* and *P. salinarum* phycospheres	Common Free-living fraction and *P. salinarum* phycospheres	Common Free-living fraction and *A. fusiformis* phycospheres
E_Methanobacteria_ Methanobacteriales	2	1						1
E_WSA2_ Methanofastidiosales	11	5	1		3		1	1
H_Halobacteria_ Halobacterales	4	1	2		1			
H_Methanomicrobia_ Methanomicrobiales	12	7	1					4
H_Methanosarcinia_ Methanosarciniales	6	3		1				2
M_Micrarchaeia_ Micrarchaeales	4	3			1			
N_Woesearchaeia_ Woesearchaeales	129	47	1		43	3	26	9
T_Thermoplasmata_ MBGD and DHVEG-1	18	9	1		4	1		3
T_Thermoplasmata_ Methanomassilicoccales	2	2						
T_Thermoplasmata_ unknown order	1	1						
Unknown Archaea	7	5						2
	196	**84**	**6**	**1**	**52**	**4**	**27**	**22**

Figure 5. (A) Phylogenetic analysis of archaeal 16S rRNA genes retrieved in *A. fusiformis* and *P. salinarum* phycospheres and in the free-living microbiome and (B) core and specific OTUs among phycospheres and free-living microbiome. The tree was constructed with ~421bp positions and rooted at mid-point. Bootstraps > 70 are presented as black circles. Occurrence of OTUs associated to the *A. fusiformis* phycosphere were presented as green squares, to the *P. salinarum* phycosphere as pink squares, while OTUs from the free-living microbiome are indicated with black squares. Abundance of OTUs was ranked as follows: 0 sequence: class 0, between 1-10 sequences: class 1, between 11-100: class 2, between 101-1000: class 3, between 1001-10000: class 4, between 10001-100000: class 5.